Editors' Suggestion

Cluster-Based Haldane State in an Edge-Shared Tetrahedral Spin-Cluster Chain: Fedotovite $K_2Cu_3O(SO_4)_3$

M. Fujihala,[1,*] T. Sugimoto,[2,†] T. Tohyama,[2] S. Mitsuda,[1] R. A. Mole,[3] D. H. Yu,[3] S. Yano,[4] Y. Inagaki,[5] H. Morodomi,[5] T. Kawae,[5] H. Sagayama,[6] R. Kumai,[6] Y. Murakami,[6] K. Tomiyasu,[7] A. Matsuo,[8] and K. Kindo[8]

[1]*Department of Physics, Faculty of Science, Tokyo University of Science, Shinjuku, Tokyo 162-8601, Japan*
[2]*Department of Applied Physics, Faculty of Science, Tokyo University of Science, Katsushika, Tokyo 125-8585, Japan*
[3]*Australian Nuclear Science and Technology Organization, Lucas Heights, New South Wales 2232, Australia*
[4]*National Synchrotron Radiation Research Center, Neutron Group, Hsinchu 30077, Taiwan*
[5]*Department of Applied Quantum Physics, Faculty of Engineering, Kyushu University, Fukuoka 819-0395, Japan*
[6]*Institute of Materials Structure Science, High Energy Accelerator Research Organization, Tsukuba, Ibaraki 305-0801, Japan*
[7]*Department of Physics, Tohoku University, Sendai 980-8578, Japan*
[8]*International MegaGauss Science Laboratory, Institute for Solid State Physics, The University of Tokyo, Kashiwa, Chiba 277-8581, Japan*

(Received 26 September 2017; published 12 February 2018)

Fedotovite $K_2Cu_3O(SO_4)_3$ is a candidate of new quantum spin systems, in which the edge-shared tetrahedral (EST) spin clusters consisting of Cu^{2+} are connected by weak intercluster couplings forming a one-dimensional array. Comprehensive experimental studies by magnetic susceptibility, magnetization, heat capacity, and inelastic neutron scattering measurements reveal the presence of an effective $S = 1$ Haldane state below $T \cong 4$ K. Rigorous theoretical studies provide an insight into the magnetic state of $K_2Cu_3O(SO_4)_3$: an EST cluster makes a triplet in the ground state and a one-dimensional chain of the EST induces a cluster-based Haldane state. We predict that the cluster-based Haldane state emerges whenever the number of tetrahedra in the EST is *even*.

DOI: 10.1103/PhysRevLett.120.077201

Quantum spin states in low-dimensional magnets have been extensively studied because of emergent spin gaps and topological features. In particular, intensive studies of one-dimensional (1D) spin systems have successfully captured the exotic quantum states such as the Tomonaga–Luttinger spin-liquid state [1] and the Haldane state [2]. The magnetic excitations of antiferromagnetic (AFM) chain systems are known to follow Haldane's conjecture: half-integer spin chains have gapless excitations, whereas spin gaps open in integer spin chains [3,4]. Furthermore, spin gaps open by interchain interactions and frustration in half-integer spin systems [5]. In fact, the spin gap in an $S = 1/2$ spin-ladder system IPA-$CuCl_3$ has been observed by neutron scattering, where two spins on a rung couple each other with ferromagnetic (FM) interactions, and thus, the Haldane gap appears [6]. The realization of such a Haldane chain has been a proposed target for a measurement-based quantum computer [7–9]. Therefore, we propose a new direction in Haldane chains based on a spin cluster in this Letter.

The Haldane state is usually constructed by integer spins and a 1D AFM interaction between them. According to preceding studies on the Haldane state in a ladder [6,10], triplet ground states in a local structure can play the role of an effective $S = 1$ spin at low temperatures. The triplet ground states can be generally realized in (i) a spin cluster consisting of an even number of $S = 1/2$ spins. Furthermore, by connecting them with (ii) a small AFM intercluster coupling, an effective Haldane chain is expected at low temperatures. To realize such a cluster-based Haldane chain, we study magnetic behaviors of an edge-shared tetrahedral (EST) spin-cluster chain (SCC) $K_2Cu_3O(SO_4)_3$, because its crystal structure seems to satisfy conditions (i) and (ii). We actually confirm the cluster-based Haldane chain in this compound based on magnetic susceptibility, magnetization, heat capacity, and inelastic neutron scattering measurements.

The synthesis of $K_2Cu_3O(SO_4)_3$ is designated after the identification of natural mineral fedotovite [11]. A single-phase polycrystalline sample is synthesized using a solid state reaction process. The space group $C2/c$ with lattice parameters of $a = 19.0948(6)$ Å, $b = 9.5282(3)$ Å, $c = 14.1860(6)$ Å, and $\beta = 110.644(3)°$ are refined by the computer program RIETAN-FP [12] [Fig. 1(a)]. These results are in good agreement with those of the natural mineral fedotovite [13].

As illustrated in Fig. 1(b), magnetic ions of Cu^{2+} form EST spin clusters, and they are connected to each other by SO_4^{2-} ions along the b axis. The interchain interactions along the a and c axes can be neglected in the experimental temperature range, because the EST-SCCs are separated along the a axis by nonmagnetic potassium ions, and

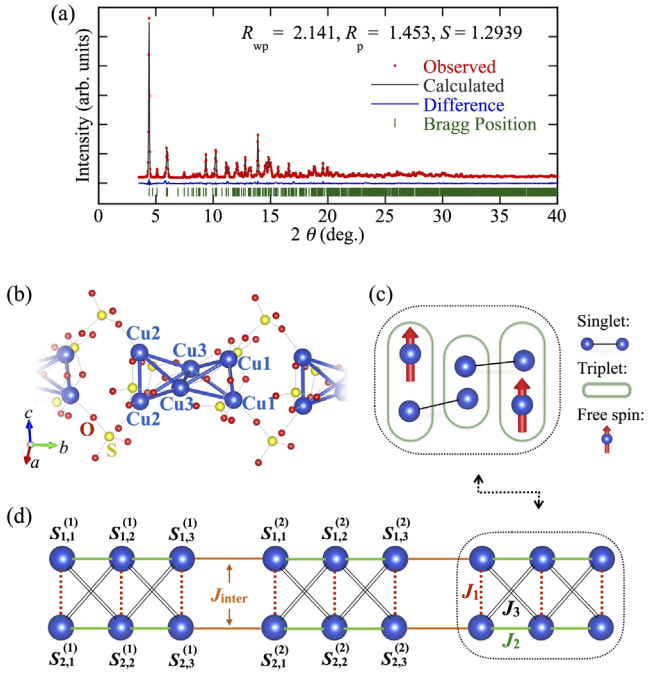

FIG. 1. (a) Rietveld refinement result of $K_2Cu_3O(SO_4)_3$ using synchrotron XRD data at room temperature. (b) The crystal structure of $K_2Cu_3O(SO_4)_3$. The EST spin cluster of the Cu^{2+} ions (blue) displayed with nearby oxygen (red) and sulfur (yellow) ions. (c) Schematic spin configuration of the $T^z = 1$ state of cluster-based $S = 1$ spin. Here, each rung composes a triplet (green oval) and antisymmetrically connects with neighbor rungs (solid line). The edge spins composing a triplet state are denoted by a red arrow. (d) An effective model for $K_2Cu_3O(SO_4)_3$. Intracluster superexchange interactions J_1 (dashed red lines), J_2 (green lines), J_3 (black double lines) in an EST spin cluster, and the intercluster interaction J_{inter} (orange lines).

the tetracoordinated Cu^{2+} ions do not have exchange paths through an anion along the c axis (see Supplemental Material Sec. II [14]). Therefore, we consider that $K_2Cu_3O(SO_4)_3$ has the near-ideal one-dimensional EST-SCCs.

In the EST cluster, the magnetic couplings originate from superexchange interactions through the Cu-O-Cu paths (see Supplemental Material Sec. II [14]). The superexchange interaction J in low-dimensional cuprates strongly depends on crystal structural parameters. According to Ref. [15], the magnetic interactions through the Cu1-O-Cu1, Cu2-O-Cu2, and Cu3-O-Cu3 paths are estimated to be small, but the magnitude of the others can be over 10 meV. We thus propose the following model Hamiltonian to describe the magnetic behaviors of $K_2Cu_3O(SO_4)_3$,

$$\mathcal{H} = \sum_{k=1}^{L-1} \mathcal{H}_{\text{inter}}^{(k:k+1)} + \sum_{k=1}^{L} \mathcal{H}_{\text{intra}}^{(k)} \tag{1}$$

with the inter- and intracluster Hamiltonians

$$\mathcal{H}_{\text{intra}}^{(k)} = J_1 \sum_{j=1,2,3} \boldsymbol{S}_{1,j}^{(k)} \cdot \boldsymbol{S}_{2,j}^{(k)} + J_2 \sum_{i=1,2} \sum_{j=1,2} \boldsymbol{S}_{i,j}^{(k)} \cdot \boldsymbol{S}_{i,j+1}^{(k)} + J_3 \sum_{j=1,2} \sum_{a=0,1} \boldsymbol{S}_{1,j+a}^{(k)} \cdot \boldsymbol{S}_{2,j+1-a}^{(k)}, \tag{2}$$

and

$$\mathcal{H}_{\text{inter}}^{(k:k+1)} = J_{\text{inter}} \sum_{i=1,2} \boldsymbol{S}_{i,3}^{(k)} \cdot \boldsymbol{S}_{i,1}^{(k+1)}, \tag{3}$$

where $\boldsymbol{S}_{i,j}^{(k)}$ is the $S = 1/2$ spin operator on the (i, j) site of kth cluster. Here, the magnitude of intercluster interaction J_{inter} is smaller than the intracluster interaction $J_{\text{intra}} = \sqrt{J_1^2 + J_2^2 + J_3^2}$. If the rung interaction J_1 is FM (or weakly AFM), the ground state of the cluster can be a triplet [see Figs. 1(c) and 1(d)], which is discussed below.

Figures 2(a), 2(b), and 2(d) present the magnetic susceptibility, inverse susceptibility, and magnetization curve of $K_2Cu_3O(SO_4)_3$. These are measured by using a superconducting quantum interference device magnetometer with a homemade ^{3}He insert [16]. The intrinsic susceptibility $\chi_{\text{bulk}}(T)$ is obtained by subtracting Pascal's diamagnetic contribution χ_{dia} [17] and Curie tail contribution $\chi_{\text{end}} = n_{\text{end}} C/(T - \theta_{\text{CW}})$ from the experimental data χ_{obs}. Here, C is the Curie constant for $S = 1/2$ with the fixed g factor as $g = 2.0$, and θ_{CW} is the Curie-Weiss temperature. As compared with the susceptibility at low temperatures $T \lesssim 3$ K in Fig. 2(a), we determine these parameters as $n_{\text{end}} = 0.032$, $C = 1.12$, and $\theta_{\text{CW}} = -0.3$ K, which should indicate 3.2% of the magnetic moment originating from free spins at the ends of the SCCs [18,19].

Figure 2(b) shows the inverse susceptibility $1/\chi_{\text{bulk}}$, which has a kink around 120 K. The Curie constants and Weiss temperatures are estimated from the $1/\chi_{\text{bulk}}$ by the Curie-Weiss law to be $C_L = 0.53$ and $\theta_L = -6.2$ K between 25 and 55 K, and to be $C_H = 1.45$ and $\theta_H = -201.4$ K between 200 and 300 K. The C_H corresponds to an effective magnetic moment of 1.97 μ_B, which is consistent with a $S = 1/2$ spin of Cu^{2+}. The Weiss temperature $\theta_H = -201.4$ K indicates that strong AFM exchange interaction dominates in this system. The ratio of C_L and C_H is 0.38, which implies that only one third of whole magnetic moments remains below 100 K. To clarify these features, we calculate the susceptibility by full diagonalization of the intracluster Hamiltonian (2) without the interchain interaction J_{inter}. As shown in Fig. 2(b), we obtain a good correspondence to experimental data with a weak FM interaction $J_1 \cong -35$ K and strong AFM interactions $J_2 = J_3 \cong 125$ K, namely, the intracluster interaction $J_{\text{intra}} = 180$ K. These parameters make the ground state of an EST spin cluster to be a triplet (discussed below).

To confirm the triplet ground state of the EST spin cluster, we measure the magnetization at high magnetic

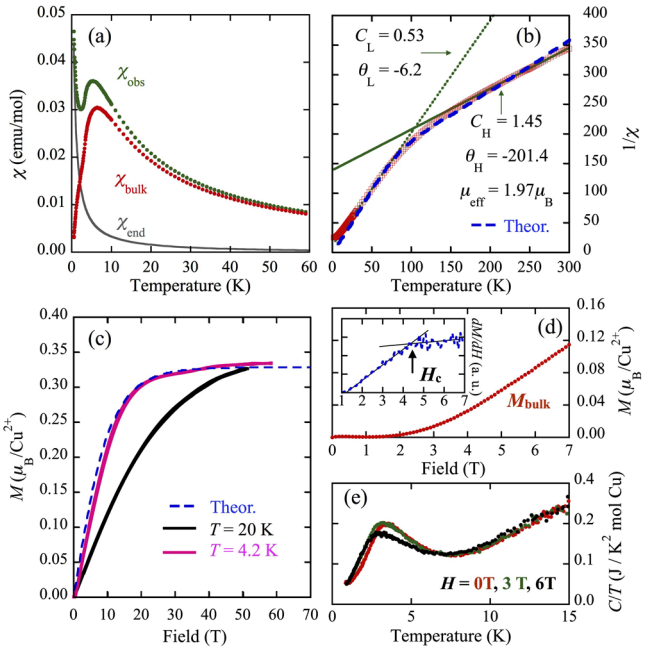

FIG. 2. (a) Temperature dependence of the magnetic susceptibility $\chi_{\rm bulk}$ (filled red circles) of $K_2Cu_3O(SO_4)_3$ measured at 0.1 T. The intrinsic susceptibility $\chi_{\rm bulk}$ is obtained by subtracting Pascal's diamagnetic contribution $\chi_{\rm dia}$ and an estimated contribution of end spins of SCCs $\chi_{\rm end}$ (gray solid line) from the experimental data $\chi_{\rm obs}$ (filled green circles). (b) The inverse susceptibility $1/\chi_{\rm bulk}$ (open red squares). The solid and broken green lines denote the fitting curves by the Curie-Weiss law. The blue dashed line represents the theoretical curve of the EST spin-cluster model (2) with a weak FM interaction $J_1 \cong -35$ K and strong AFM interactions $J_2 = J_3 \cong 125$ K. (c) High-field magnetization at 4.2 K (pink solid line) and 20 K (black solid line). The blue dashed line denotes the theoretical magnetization curve obtained in the EST spin-cluster model with the same parameters in (b). (d) The magnetization of bulk $M_{\rm bulk}$ (filled red circles) and its field derivative $dM_{\rm bulk}/dH$ (inset) measured at 0.52 K. The black solid lines are a guide to the eye. (e) The temperature dependence of the total specific heat divided by temperature C/T for 0, 3, and 6 T.

fields of up to 58 T. We can see a good coincidence between the theoretical and experimental data [see Fig. 2(c)], where the one-third plateau appears with a small magnetic field as compared with the AFM interactions $J_2 = J_3 \cong 125$ K. The good agreement strongly suggests that a spin-triplet state exists in $K_2Cu_3O(SO_4)_3$ in the high-temperature region. Therefore, the Haldane state is expected to be realized in the low-temperature region.

Next, we consider the intercluster effect in $K_2Cu_3O(SO_4)_3$. The intrinsic magnetization $M_{\rm bulk}(H)$ is also obtained by subtracting the contribution of end spins of SCCs from the experimental data by using the following equation $n_{\rm end} g S \mu_B [2\coth(gS\mu_B H/k_B T) - \coth(gS\mu_B H/2k_B T)]$ [Fig. 2(d)]. The $M_{\rm bulk}(H)$ shows $M = 0$ plateau, which indicates the existence of a spin gap. The critical field value H_c and the energy gap Δ_{MH} are related by the following equation $g\mu_B H_c = \Delta_{MH}$. The inset in Fig. 2(d) shows the field derivative of the magnetization curve $dM_{\rm bulk}/dH$. A continuous transition can be seen at $H_c \approx 4.5$ T. Therefore, the excitation gap is obtained as $\Delta_{MH} \approx 6$ K.

The existence of the spin gap in $K_2Cu_3O(SO_4)_3$ is also supported by magnetic susceptibility and specific heat measurements [Fig. 2(a) and 2(e)]. The $\chi_{\rm bulk}$ shows a broad maximum at around 4 K and a decrease to zero with decreasing temperature. At the same temperature, a Schottky-like peak in the heat capacity is observed. This peak corresponds to an energy gap $\Delta \approx 10$ K in a two-level approximation. If the two levels originate from the triplet and singlet of a local structure, the Schottky peak should show a field-sensitive gradual feature due to Zeeman splitting [20]. However, such a feature is not observed in the specific heat, as shown in Fig. 2(e), and thus a local triplet-singlet gap does not explain the Schottky-like peak.

To confirm the observation of the spin gap and to determine its magnitude, we performed an inelastic neutron scattering (INS) measurement. Data were acquired using the cold-neutron time-of-flight spectrometer PELICAN. The INS data (Fig. 3(a)) show a gapped spectrum at 1.5 K, with no evidence of a quasielastic signal below the gap, and a characteristic of end spins in Haldane chains is observed [21]. Measurements taken at 4 K show that the spin gap has closed, though the remaining intensity is broad in both Q and E. This response is typical of short-range correlations in a 1D chain. Inspection of the elastic line reveals no additional Bragg reflections, showing that there is no magnetic long-range order. The lower bound of the gap corresponds to a $\Delta_{\rm INS} = 0.61(3)$ meV $= 7.1$ K. This is consistent with that determined by magnetization. The observation of dispersive modes in the INS data is consistent with $K_2Cu_3O(SO_4)_3$ being highly one dimensional. A general feature of powder averaged data is that the zone boundary contributions are dominant. One consequence of this is that the observed dispersion minima are slightly off from the Brillouin zone centers π/b and $3\pi/b$ to the high-Q side. However, it is reasonable to assume that this is the

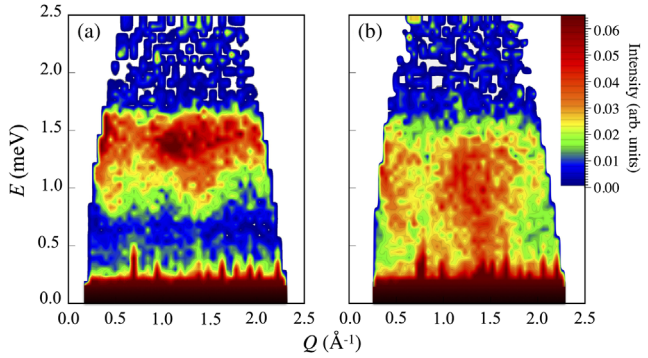

FIG. 3. The INS data by time-of-flight method in $K_2Cu_3O(SO_4)_3$, measured at (a) 1.5 and (b) 4.0 K.

powder averaged spectrum, where the excitations only disperse along one crystallographic direction [22,23]. Therefore, we conclude that the ground state of $K_2Cu_3O(SO_4)_3$ is a cluster-based Haldane state.

Finally, we discuss the cluster-based Haldane state from a theoretical point of view and estimate the intercluster interaction. The cluster-based $S = 1$ spin operators in the kth cluster $\boldsymbol{T}_k$ are analytically obtained by triplet ground states of the cluster [24]. Figure 1(c) shows a schematic configuration of the $T^z = 1$ state of the cluster-based $S = 1$ spin. The projection operator on the triplet states $\mathcal{P}^{(k)}$ gives us a relation between the edge spins $\boldsymbol{S}_{i,j}^{(k)}$ ($i = 1$, 2 and $j = 1, 3$) and the cluster-based spin: $\mathcal{P}^{(k)}\boldsymbol{S}_{i,j}^{(k)}\mathcal{P}^{(k)} = \frac{3}{8}\boldsymbol{T}_k$ for $i = 1$, 2 and $j = 1$, 3. Therefore, we obtain the cluster-based Haldane chain as follows:

$$\mathcal{H}_{\mathrm{eff}} = \mathcal{P}\mathcal{H}\mathcal{P} = J_{\mathrm{eff}}\sum_k \boldsymbol{T}_k \cdot \boldsymbol{T}_{k+1} + \mathrm{const}, \qquad (4)$$

where the projection is given by $\mathcal{P} = \prod_k \mathcal{P}^{(k)}$ and the effective exchange energy J_{eff} between cluster-based $S = 1$ spins [see Fig. 4(a)] corresponds to $9J_{\mathrm{inter}}/32$. In this effective model, the Haldane gap in the thermodynamical limit is obtained to be $\Delta_{\mathrm{eff}} \sim 0.41J_{\mathrm{eff}} \cong 0.12J_{\mathrm{inter}}$ [25],

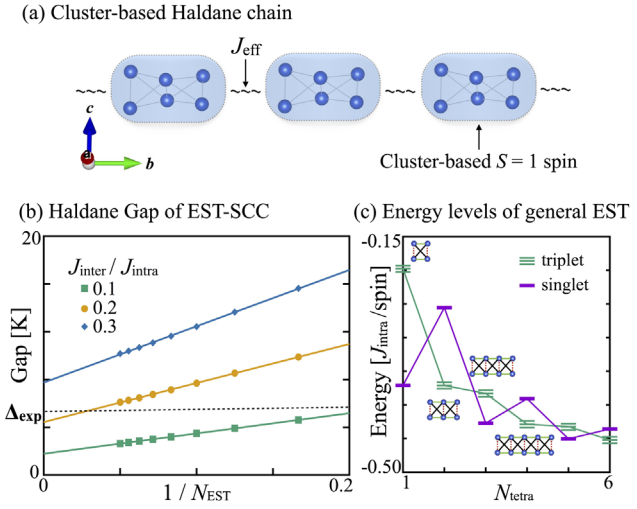

FIG. 4. (a) Schematic effective model of cluster-based $S = 1$ Haldane chain. Each cluster composes a cluster-based $S = 1$ spin, and the effective exchange interaction originates from the intercluster interaction. (b) Extrapolation of the Haldane gaps as a function of inverse system size N_{EST} for various J_{inter}. The Haldane gap is defined by the energy gap between $M = 1$ and 2 ground states. The black dashed line indicates the magnitude of the gap obtained by the INS experiment. (c) Ground-state energies of singlet and triplet versus number of tetrahedra in a generalized EST spin cluster. Here, we neglect intercluster interaction and use the same intracluster superexchange interactions as the estimated values for $K_2Cu_3O(SO_4)_3$ corresponding to the case of $N_{\mathrm{tetra}} = 2$.

when the intercluster interaction J_{inter} is much smaller than the intracluster interaction J_{intra}.

Figure 4(b) shows the Haldane gap as a function of inverse system size $1/N_{\mathrm{EST}}$ for various $J_{\mathrm{inter}}/J_{\mathrm{intra}} = 0.1$, 0.2, and 0.3, which are numerically obtained by the variational matrix-product state method [26] in the model Hamiltonian (1) with the intracluster interaction $J_{\mathrm{intra}} = 180$ K. We can confirm that the Haldane gap $\Delta_{\mathrm{calc}} \sim 2.2$ K in the thermodynamical limit $N_{\mathrm{EST}} \to \infty$ for $J_{\mathrm{inter}} = 0.1$ $J_{\mathrm{intra}} = 18$ K corresponds to Δ_{eff} obtained in the effective model, and therefore the numerical result verifies emergence of the cluster-based Haldane state for a small intercluster interaction. By comparing with the gap obtained by the INS experiment $\Delta_{\mathrm{INS}} \cong 7$ K, the intercluster interaction in $K_2Cu_3O(SO_4)_3$ is roughly estimated to be $J_{\mathrm{inter}} \cong 0.2J_{\mathrm{intra}} \cong 36$ K. Since the estimated intercluster interaction is small enough as compared with the intracluster interaction, we conclude that the low-temperature state of $K_2Cu_3O(SO_4)_3$ is in the condition for the cluster-based Haldane state.

Furthermore, we propose an extension of our model to general EST-SCCs where the number of tetrahedra N_{tetra} in the EST cluster is adjustable. The isolated tetrahedra and frustrated spin-ladder systems can be regarded as the $N_{\mathrm{tetra}} = 1$ and ∞ cases, since an EST cluster is regarded as a two-leg ladder with a diagonal second-neighbor interaction, and they have been studied in several synthesized materials [27–29]. If the exchange energy J_1 is smaller than AFM J_2 and J_3, the spin configuration of a rung corresponds to the triplet (symmetric). The AFM leg and diagonal interactions require an antisymmetric configuration between neighboring rungs, and thus the ground state of an EST cluster alternates between singlet and triplet by increasing the number of tetrahedra N_{tetra} [see Fig. 4(c)]. Consequently, we conclude that the cluster-based Haldane state is realized in the general EST-SCCs when the number of tetrahedra is even, i.e., $N_{\mathrm{tetra}} = 0 \pmod 2$.

In summary, we have found that fedotovite $K_2Cu_3O(SO_4)_3$ has a unique arrangement of magnetic ions and a two-stage magnetic behavior divided by a characteristic temperature $T \cong 4$ K. The high-temperature experiments have given good correspondence to theoretical thermodynamical values of an EST spin cluster whose ground state is a triplet based on the Haldane state in a three-rung ladder. In the lower-temperature region, the experimental data indicate the existence of a spin gap, which is expected by the cluster-based $S = 1$ Haldane state. Furthermore, we have theoretically obtained an effective Hamiltonian of a cluster-based $S = 1$ Haldane chain and estimated the intercluster interaction of $K_2Cu_3O(SO_4)_3$ by comparing the spin gap observed in the INS experiment. Our study can propose an extension of general EST-SCCs exhibiting the cluster-based $S = 1$ Haldane state when the number of tetrahedra is even. Since recent studies on measurement-based quantum computation have presented

some merits of the Haldane state [7–9], $K_2Cu_3O(SO_4)_3$, as well as general EST-SCCs, is a promising candidate of resource state and an important example as a designable cluster-based quantum computer [30].

Travel expenses for the inelastic neutron scattering experiments performed using PELICAN at ANSTO, Australia, were supported by General User Program for Neutron Scattering Experiments, Institute for Solid State Physics, The University of Tokyo (Proposal No. 16900), at JRR-3, Japan Atomic Energy Agency, Tokai, Japan. Synchrotron powder XRD measurements were performed with the approval of the Photon Factory Program Advisory Committee (Proposals No. 2015P001 and No. 2016G030). T. S. and T. T. were supported by Priority Issue (creation of new functional devices and high-performance materials to support next-generation industries) to be tackled by using Post 'K' Computer, MEXT, Japan. Numerical calculation in this work was carried out on the supercomputers at JAEA and the Supercomputer Center at Institute for Solid State Physics, University of Tokyo. This study is partly supported by the Grant-in-Aid for Scientific Research (Nos. 17K14344, 16K17753, JP17H06137, and JP15H03692) from MEXT, Japan.

*fujihara@nsmsmac4.ph.kagu.tus.ac.jp
†sugimoto.takanori@rs.tus.ac.jp

[1] I. A. Zaliznyak, Nat. Mater. **4**, 273 (2005).
[2] I. Affleck, J. Phys. Condens. Matter **1**, 3047 (1989).
[3] F. D. M. Haldane, Phys. Rev. Lett. **50**, 1153 (1983).
[4] F. D. M. Haldane, Phys. Lett. **93A**, 464 (1983).
[5] T. M. Rice, S. Gopalan, and M. Sigrist, Europhys. Lett. **23**, 445 (1993).
[6] T. Masuda, A. Zheludev, H. Manaka, L.-P. Regnault, J.-H. Chung, and Y. Qiu, Phys. Rev. Lett. **96**, 047210 (2006).
[7] D. Gross and J. Eisert, Phys. Rev. Lett. **98**, 220503 (2007).
[8] G. K. Brennen and A. Miyake, Phys. Rev. Lett. **101**, 010502 (2008); A. Miyake, Phys. Rev. Lett. **105**, 040501 (2010).
[9] D. V. Else, I. Schwarz, S. D. Bartlett, and A. C. Doherty, Phys. Rev. Lett. **108**, 240505 (2012).
[10] T. Vekua and A. Honecker, Phys. Rev. B **73**, 214427 (2006).
[11] L. P. Vergasova, S. K. Filatov, Y. K. Serafimova, and G. L. Starova, Sov. Phys. Dokl. **299**, 961 (1988).
[12] F. Izumi and K. Momma, Solid State Phenom. **130**, 15 (2007).
[13] G. L. Starova, S. K. Filatov, V. S. Fundamensky, and L. P. Vergasova, Mineral Mag. **55**, 613 (1991).
[14] See Supplemental Material at http://link.aps.org/supplemental/10.1103/PhysRevLett.120.077201 for the experimental details and crystal structure.
[15] Y. Mizuno, T. Tohyama, S. Maekawa, T. Osafune, N. Motoyama, H. Eisaki, and S. Uchida, Phys. Rev. B **57**, 5326 (1998).
[16] Y. Sato, S. Makiyama, Y. Sakamoto, T. Hasuo, Y. Inagaki, T. Fujiwara, H. S. Suzuki, K. Matsubayashi, Y. Uwatoko, and T. Kawae, Jpn. J. Appl. Phys. **52**, 106702 (2013).
[17] G. A. Bain and J. F. Berry, J. Chem. Educ. **85**, 532 (2008).
[18] No evidence of an impurity phase is observed in the synchrotron XRD patterns [see Fig. 1(a)]. Therefore, the low-temperature Curie tail should be caused by the end spins of SCCs as well as the $S = 1$ Haldane chain compound, $Ni(C_3H_{10}N_2)_2N_3(ClO_4)$ [19].
[19] G. E. Granroth, S. Maegawa, M. W. Meisel, J. Krzystek, L.-C. Brunel, N. S. Bell, J. H. Adair, B. H. Ward, G. E. Fanucci, L.-K. Chou, and D. R. Talham, Phys. Rev. B **58**, 9312 (1998).
[20] M. Fujihala, X. G. Zheng, H. Morodomi, T. Kawae, A. Matsuo, K. Kindo, and I. Watanabe, Phys. Rev. B **89**, 100401(R) (2014).
[21] M. Kenzelmann, G. Xu, I. A. Zaliznyak, C. Broholm, J. F. DiTusa, G. Aeppli, T. Ito, K. Oka, and H. Takagi, Phys. Rev. Lett. **90**, 087202 (2003).
[22] M. B. Stone, G. Ehlers, and G. E. Granroth, Phys. Rev. B **88**, 104413 (2013).
[23] G. J. Nilsen, A. Raja, A. A. Tsirlin, H. Mutka, D. Kasinathan, C. Ritter, and H. M. Rønnow, New J. Phys. **17**, 113035 (2015).
[24] More explicitly, the cluster-based $S = 1$ spin operators are given by $T^z_k = \sum_{\alpha=\pm,0}\alpha|\alpha^{(k)}\rangle\langle\alpha^{(k)}|$ and $T^{\pm}_k = \sqrt{2}(|\pm^{(k)}\rangle\langle 0^{(k)}| + |0^{(k)}\rangle\langle\pm^{(k)}|)$ where $|\alpha^{(k)}\rangle$ ($\alpha = \pm$ or 0) denotes the triplet ground state as the Haldane state in the kth cluster. In this expression, the projection operator is also given by $\mathcal{P}^{(k)}K = \sum_{\alpha=\pm,0}|\alpha^{(k)}\rangle\langle\alpha^{(k)}|$.
[25] S. R. White, Phys. Rev. Lett. **69**, 2863 (1992).
[26] U. Schollwöch, Ann. Phys. (Amsterdam) **326**, 96 (2011).
[27] P. Lemmens, K.-Y. Choi, E. E. Kaul, C. Geibel, K. Becker, W. Brenig, R. Valenti, C. Gros, M. Johnsson, P. Millet, and F. Mila, Phys. Rev. Lett. **87**, 227201 (2001).
[28] M. Fujihala, X. G. Zheng, H. Morodomi, T. Kawae, and I. Watanabe, Phys. Rev. B **87**, 144425 (2013).
[29] A. Zheludev, V. O. Garlea, L. P. Regnault, H. Manaka, A. Tsvelik, and J.-H. Chung, Phys. Rev. Lett. **100**, 157204 (2008).
[30] F. Meier, J. Levy, and D. Loss, Phys. Rev. Lett. **90**, 047901 (2003).